J. Phase Equilib. Diffus. (2021) 42:77–90
https://doi.org/10.1007/s11669-020-00859-5

Thermodynamic Descriptions of the Co–Zr and Co–Fe–Zr Systems

Chenyang Zhou[1] · **Hang Wang**[1]

Submitted: 12 October 2020 / in revised form: 17 November 2020 / Accepted: 10 December 2020 / Published online: 3 January 2021

Abstract The Co–Fe–Zr system and its Co–Zr subsystem were optimized using the CALculation of PHAse Diagram (CALPHAD) approach. The substitutional solution model was used for describing the phases liquid, fcc_A1, bcc_A2 and hcp_A3. Two Laves phases were modeled as $(Co,Fe,Zr)_2(Co,Fe,Zr)_1$, and the phases CoFe and CoZr with the bcc_B2 crystal structure were described as the ordered one of bcc_A2 in the formula $(Co,Fe,Va,Zr)_{0.5}(Co,Fe,Va,Zr)_{0.5}Va_3$. With limited solubility ranges, all other phases were treated as the line compounds $(Co,Fe)_mZr_n$. An excellent agreement between the reported and calculated results was reached. The reliable thermodynamic parameters of the Co–Fe–Zr system were acquired, which can be well applied to various thermodynamic calculations and materials design.

Keywords Co–Zr system · Co–Fe–Zr system · CALPHAD · phase diagram

1 Introduction

The Co–Fe–Zr system is a basic and key system in hydrogen storage materials, amorphous alloys, high-entropy alloys, and magnetic materials.

In the international thermonuclear experimental reactor (ITER) project, the intermetallic compound ZrCo is intended to replace uranium for the storage and delivery of tritium.[1] Fe substitution for Co can enhance the durability against the hydrogen-induced disproportionation, which makes it more favorable to store tritium.[2] And cobalt, iron and zirconium are the principal elements in amorphous alloys[3–6] and high-entropy alloys.[7–9] Furthermore, Hoque et al.[10] have reported a two-phase magnetic $Co_{11}Zr_2$–$Co_{23}Zr_6$ system and the addition of Fe can improve its magnetic and mechanical properties.

The further development of such novel materials is largely dependent on the accurate phase equilibria information and detailed thermodynamic description of the Co–Fe–Zr system. Recently, the Co–Fe–Zr isothermal sections between 1273 and 1573 K have been experimentally studied by Wang et al.[11], and the Co–Fe, Co–Zr and Fe–Zr subsystems have been thermodynamically assessed by several researchers.[12–14] Whereas the Co–Zr thermodynamic parameters.[13] still need to be adjusted because of the inappropriate thermodynamic model of CoZr and low-temperature decomposition of $CoZr_3$. As a result, the current study is aimed to develop reasonable thermodynamic descriptions and obtain a self-consistent set of thermodynamic parameters for the Co–Zr and Co–Fe–Zr systems using the CALPHAD approach.

2 Literature Review

2.1 Co–Fe System

Guillermet,[15] Ohnuma et al.[16] and Turchanin et al.[17] carried out the thermodynamic studies of the Co–Fe system, but their calculated magnetic properties did not completely reproduce the experimental data.[18–20] Wang et al.[12] conducted the first-principles calculations and heat

✉ Chenyang Zhou
zhoucy@jxust.edu.cn

[1] Faculty of Materials Metallurgy and Chemistry, Jiangxi University of Science and Technology, Ganzhou 341000, Jiangxi, People's Republic of China

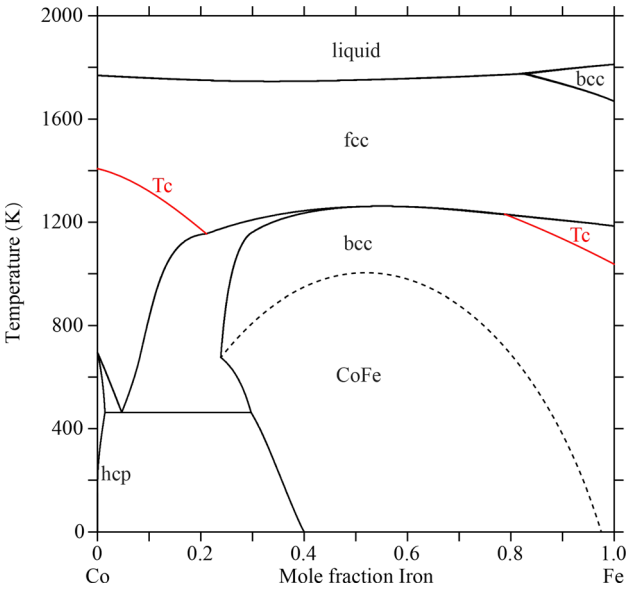

Fig. 1 Co–Fe phase diagram assessed by Wang et al.[12]

capacity measurements and performed a detailed thermodynamic assessment of the Co–Fe system. Their thermodynamic parameters[12] are directly adopted in the current work. Fig. 1 presents the Co–Fe phase diagram assessed by Wang et al.[12]

2.2 Co–Zr System

Chart and Putland,[21] Saunders and Miodownik[22] and Bratberg and Jansson[23] performed the early thermodynamic optimizations of the Co–Zr system, but the thermochemical data were not considered in their work. Liu et al.[24] carried out the detailed experimental determination and proper thermodynamic assessment of the Co–Zr system; however, the reported mixing enthalpies of liquid phase[25–27] were still not taken into consideration. Durga and Kumar[28] first coupled bcc_A2 and CoZr using an order-disorder model and improved the Co–Zr thermodynamic description. Kosorukova et al.[29] and Semenova et al.[30] performed the experimental investigations on the controversial part of the Co–Zr phase diagram including the phase transition and phase stability of $CoZr_3$. Given the available phase equilibria and thermochemical information[24–37], Agraval et al.[13] conducted a novel Co–Zr thermodynamic assessment. Nevertheless, the thermodynamic parameters of CoZr and $CoZr_3$[13] still required to be revised to match the common model of the order-disorder transition and avoid the low-temperature decomposition of $CoZr_3$. As a result, the Co–Zr thermodynamic modeling is updated in this work.

The Co–Zr phase diagram was first studied by Pechin et al.,[31] who identified the five compounds $Co_{11}Zr_2$, Co_4Zr (also called as $Co_{23}Zr_6$), λ_2, CoZr and $CoZr_2$. Bataleva et al.[32] used metallography, EPMA, XRD and DTA to carry out the experimental study on the Co–Zr phase diagram, especially the liquidus temperatures. The reported phase diagrams[31, 32] were contradictory in the Zr-rich part owing to the presence of $CoZr_3$[32]. Liu et al.[24] adopted the same method as Bataleva et al.[32] to measure the phase equilibria of the Co–Zr system in the complete composition ranges above 1073 K. $CoZr_3$ was found to form peritectically from liquid + bcc_A2 at 1253 K,[32] but peritectoidically from $CoZr_2$ + bcc_A2 at 1254 K.[24] Kosorukova et al.[29] also reported the temperatures of four invariant reactions using metallography, XRD and DTA. Semenova et al.[30] determined the $CoZr_2$–Zr region of the Co–Zr phase diagram using the same methods as Kosorukova et al.,[29] and their experimental results supported the conclusion[24] that $CoZr_3$ formed by the peritectoid reaction $CoZr_2$ + bcc_A2 → $CoZr_3$ at 1254 K. For the development of the present description, all phase equilibria data[24, 29–32] are considered.

The enthalpies of formation of the Co–Zr compounds were studied by several researchers using direct synthesis reaction calorimetry[33, 34], differential calorimetry,[35] solution calorimetry[36] and first-principles calculations[37]. In the update process, the reported thermochemical data related to CoZr, $CoZr_2$ and $CoZr_3$ are taken into consideration.

2.3 Fe–Zr System

The early thermodynamic studies of the Fe–Zr system were performed by Servant et al.[38] and Jiang et al.[39] The Fe–Zr phase diagram was measured using metallography, EPMA, XRD and DTA by Stein et al.,[40] who suggested that $Fe_{23}Zr_6$ should be a metastable phase and its existence in the Fe–Zr system was mainly due to the stabilization of oxygen. Guo et al.[41] accepted their experimental results[40] and then performed a new thermodynamic assessment of the Fe–Zr system. But Yang et al.[42] and Lu et al.[43] thought $Fe_{23}Zr_6$ as a stable phase and re-modeled the Fe–Zr system. Saenko et al.[14] considered the experimental and theoretical thermochemical properties,[44–46] determined the heat capacity of $FeZr_2$ from 220 to 450 K, agreed with Stein et al.[40] that $Fe_{23}Zr_6$ was not an equilibrium phase, and carried out the thermodynamic remodeling of the Fe–Zr system. Their calculated results reproduced the experimental data better, hence the thermodynamic parameters of Saenko et al.[14] are directly

adopted in this work. Fig. 2 is the Fe–Zr phase diagram assessed by Saenko et al.[14]

2.4 Co–Fe–Zr System

The isothermal section of the Co–Fe–Zr system at 1273 K was reported by Panteleimonov et al.,[47] Two continuous solid solutions (Co,Fe)Zr_2 and λ_2 and three three-phase regions (Co,Fe)Zr_2 + λ_2 + CoZr, λ_2 + Co_4Zr + Fe_3Zr and Co_4Zr + Fe_3Zr + fcc(Co,Fe) were identified, but the stability of $FeZr_2$ was inconsistent with that in the Fe–Zr system[40]. Mishenina et al.[48] investigated some equilibrated alloys to determine the Co–Fe–Zr isothermal section at 770 K, but the $FeZr_2$ stability was also in discrepancy with that in the Fe–Zr system[40]. In addition, Mishenina et al.[48] did not report the bcc_A2/CoFe phase boundaries from the Co–Fe system and the occurrence of $Co_{11}Zr_2$ and $CoZr_3$. Wang et al.[11] measured four isothermal sections in the entire composition ranges at 1273, 1373, 1473 and 1573 K utilizing metallography, EPMA, XRD and DSC, in which liquid and λ_2 formed the continuous solid solutions between 1273 and 1573 K from the Co–Zr to Fe–Zr corner. Four reported isothermal sections[11] are in good accordance with the corresponding subsystems and thus accepted in the optimization process.

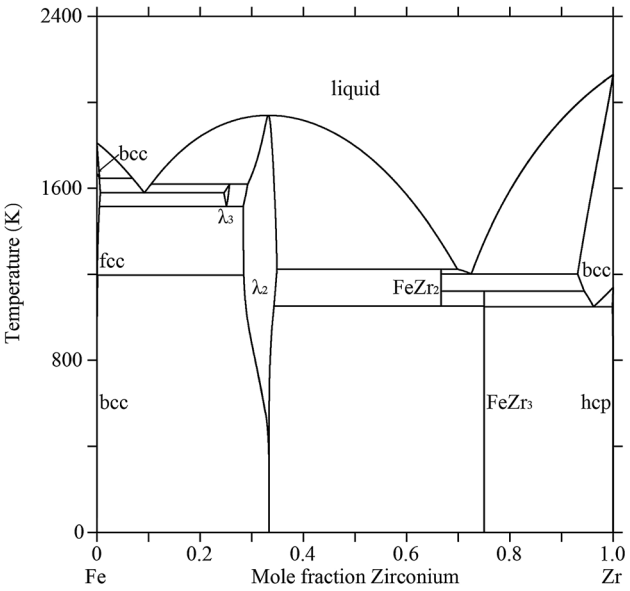

Fig. 2 Fe–Zr phase diagram assessed by Saenko et al.[14]

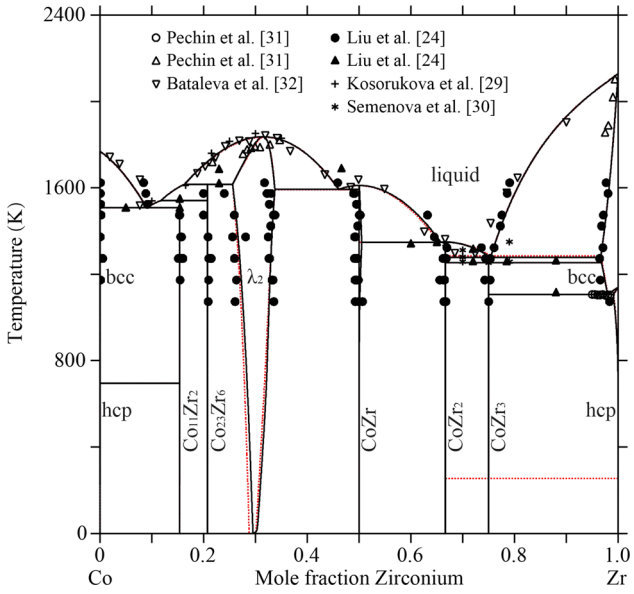

Fig. 3 Calculated Co–Zr phase diagram (solid line) compared with the previous work[13] (dotted line) and experimental data.[21, 26–29]

Table 1 The crystal structures and thermodynamic models of each phase in the Co–Fe–Zr system

Phase	Strukturbericht designation	Pearson symbol	Space group	Prototype	Thermodynamic model
Liquid	…	…	…	…	$(Co,Fe,Zr)_1$
fcc(Co,Fe)	*A*1	*cF4*	$Fm\bar{3}m$	Cu	$(Co,Fe,Zr)_1Va_1$
hcp(Co,Zr)	*A*3	*hP2*	$P63/mmc$	Mg	$(Co,Fe,Zr)_1Va_{0.5}$
bcc(Fe,Zr)	*A*2	*cI2*	$Im\bar{3}m$	W	$(Co,Fe,Va,Zr)_1Va_3$
CoFe/CoZr	*B*2	*cP2*	$Pm\bar{3}m$	CsCl	$(Co,Fe,Va,Zr)_{0.5}(Co,Fe,Va,Zr)_{0.5}Va_3$
$Co_{11}Zr_2$	…	…	…	…	$(Co,Fe)_{11}Zr_2$
$(Co,Fe)_{23}Zr_6$	$D8_a$	*cF116*	$Fm\bar{3}m$	$Mn_{23}Th_6$	$(Co,Fe)_{23}Zr_6$
λ_2	*C*15	*cF24*	$Fd\bar{3}m$	$MgCu_2$	$(Co,Fe,Zr)_2(Co,Fe,Zr)_1$
$(Co,Fe)_1Zr_2$	*C*16	*tI12*	$I4/mcm$	Al_2Cu	$(Co,Fe)_1Zr_2$
$(Co,Fe)_1Zr_3$	$E1_a$	*oC16*	*Cmcm*	Re_3B	$(Co,Fe)_1Zr_3$
λ_3	*C*36	*hP24*	$P63/mmc$	$MgNi_2$	$(Co,Fe,Zr)_2(Co,Fe,Zr)_1$

Table 2 The invariant reactions in the Co–Zr system

Invariant reaction	T,(K)	Compositions (at.%Zr)			References
		Phase 1	Phase 2	Phase 3	
liq. → fcc(Co) + $Co_{11}Zr_2$	1507	9.0	0.01	15.4	This work
					13
	1503	9.5	…	…	31
	1513	9.0	…	…	32
	1503	…	…	…	24
liq. + $Co_{23}Zr_6$ → $Co_{11}Zr_2$	1540	11.8	20.7	15.4	This work
					13
	1543	…	…	…	31
	1543	…	…	…	32
	1544	…	…	…	24
	1553	…	…	…	29
liq. + λ_2 → $Co_{23}Zr_6$	1615	16.3	25.6	20.7	This work
	1723	…	…	…	31
	1623	…	…	…	32
	1616	…	…	…	24
	1615	16.3	25.6	20.7	13
liq. → λ_2	1836	31.5	31.5	…	This work
	1833	…	…	…	32
	1835	31.5	31.5	…	13
liq. → λ_2 + CoZr	1592	46.1	33.8	50.0	This work
	1583	46.6	…	…	31
	1533	46.0	…	…	32
	1586	…	…	…	24
	1591	46.1	33.8	50.0	13
liq. → CoZr	1610	50.0	50.0	…	This work
	1643	…	…	…	32
	1610	50.0	50.0	–	13
liq. → CoZr + $CoZr_2$	1348	65.8	50.5	66.7	This work
	1333	65.0	…	…	31
	1313	64.0	…	…	32
	1337	…	…	…	24
	1348	65.5	50.0	66.7	13
liq. → $CoZr_2$	1349	66.7	66.7	…	This work
	1363	…	…	…	32
	1343	…	…	…	30
	1349	66.7	66.7	…	13
liq. → $CoZr_2$ + bcc(Zr)	1279	75.4	66.7	96.6	This work
	1253	78.5	…	…	31
	1258	…	…	…	24
	1303	75.4	…	…	29
	1259	78.0	…	…	30
	1284	75.5	66.7	96.7	13
fcc(Co) + $Co_{11}Zr_2$ → hcp(Co)	695	0.01	15.4	0.01	This work
					13
$CoZr_2$ + bcc(Zr) → $CoZr_3$	1254	66.7	96.8	75.0	This work
	1254	…	…	…	24
	1251	…	…	…	29
	1254	…	…	…	30
	1254	66.7	96.9	75.0	13
bcc(Zr) → $CoZr_3$ + hcp(Zr)	1106	97.9	75.0	99.0	This work
	1103	…	…	…	32
	1111	…	…	…	24
	1103	…	…	…	29
	1106	98.0	75.0	99.1	13

Table 3 The enthalpies of formation of the Co–Zr compounds

Phase	*T*, K	Enthalpies of formation (J/mol of atoms)	References
$Co_{11}Zr_2$	298	−23944	13, This work
$Co_{23}Zr_6$	1596	−29800 ± 1500	33
λ_2	0	−21900	37
	298	−28642	13, This work
	1708	−41000 ± 1600	33
	298	−37667 ± 3667	36
	298	−35800 ± 600	34
	0	−31680	37
	298	−31920	13
	1708	−37261	This work
	298	−31775	This work
CoZr	1512	−42200 ± 1000	33
	1030	−43050 ± 3900	35
	298	−35800 ± 700	34
	0	−28830	37
	298	−35326	13
	1512	−40267	This work
	298	−35694	This work
$CoZr_2$	1290	−33000 ± 2000	33
	298	−26400 ± 1000	34
	0	−26300	37
	298	−30745	13
	1290	−32547	This work
	298	−28946	This work
$CoZr_3$	0	−22440	37
	298	−23010	13, This work

3 Thermodynamic Models

3.1 Unary Phases

The lattice stability parameters of Co, Fe and Zr were taken from the SGTE Pure 5.1 Database.[49]

3.2 Solution Phases

The substitutional solution model was adopted to describe the solution phases ϕ (ϕ = liquid, fcc_A1, bcc_A2 and hcp_A3):

$$G_m^{\phi}(T) = \sum_i x_i G_i^{\phi}(T) + RT\sum_i x_i \ln x_i + {}^{E}G_m^{\phi} + {}^{mag}G_m^{\phi} \quad \text{(Eq 1)}$$

where x_i represents the molar fraction of i (i = Co, Fe, Zr); means the excess Gibbs energy, generally expanded using a Redlich–Kister type polynomial;[50] ${}^{mag}G_m^{\phi}$ presents the magnetic part of the Gibbs energy, expanded using a Hillert-Jarl type formalism.[51]

$$\begin{aligned} {}^{E}G_m^{\phi} =& x_{Co}x_{Fe}\sum_j {}^{j}L_{Co,Fe}^{\phi}(x_{Co}-x_{Fe})^j \\ &+ x_{Co}x_{Zr}\sum_j {}^{j}L_{Co,Zr}^{\phi}(x_{Co}-x_{Zr})^j \\ &+ x_{Fe}x_{Zr}\sum_j {}^{j}L_{Fe,Zr}^{\phi}(x_{Fe}-x_{Zr})^j \\ &+ x_{Co}x_{Fe}x_{Zr}({x_{Co}}^{0}L_{Co,Fe,Zr}^{\phi} \\ &+ {x_{Fe}}^{1}L_{Co,Fe,Zr}^{\phi} + {x_{Zr}}^{2}L_{Co,Fe,Zr}^{\phi}) \end{aligned} \quad \text{(Eq 2)}$$

where the jth interaction parameters ${}^{j}L_{Co,Fe}^{\phi}$, ${}^{j}L_{Co,Zr}^{\phi}$, ${}^{j}L_{Fe,Zr}^{\phi}$, ${}^{j}L_{Co,Fe,Zr}^{\phi}$ are taken from Refs.[12–14] or optimized in the present work.

3.3 Intermetallic Phases

Two Laves phases were described as $(Co,Fe,Zr)_2$(-Co,Fe,Zr)$_1$ using a usual two-sublattice model. Moreover, four intermetallic phases $Co_{11}Zr_2$, $(Co,Fe)_{23}Zr_6$, $(Co,Fe)_1$-Zr_2 and $(Co,Fe)_1Zr_3$ were modeled as the line compounds in the formula $(Co,Fe)_mZr_n$ due to their limited

Table 4 The thermodynamic parameters in the Co–Fe–Zr system

Phase	Thermodynamic parameters	References
Liquid	${}^{0}L^{\text{liq.}}_{\text{Co,Fe}} = -9939.0 + 3.2900T$	12
	${}^{1}L^{\text{liq.}}_{\text{Co,Fe}} = -1713.0 + 0.9100T$	12
	${}^{2}L^{\text{liq.}}_{\text{Co,Fe}} = +1271.0$	12
	${}^{0}L^{\text{liq.}}_{\text{Co,Zr}} = -145951.0 + 20.0000T$	13
	${}^{1}L^{\text{liq.}}_{\text{Co,Zr}} = -12061.8 - 5.3370T$	13
	${}^{2}L^{\text{liq.}}_{\text{Co,Zr}} = +5415.8$	13
	${}^{0}L^{\text{liq.}}_{\text{Fe,Zr}} = -85196.3 + 12.8300T$	14
	${}^{1}L^{\text{liq.}}_{\text{Fe,Zr}} = -1655.5$	14
	${}^{0}L^{\text{liq.}}_{\text{Co,Fe,Zr}} = -110919.3 + 83.1767T$	This work
	${}^{1}L^{\text{liq.}}_{\text{Co,Fe,Zr}} = -172919.3 + 83.1767T$	This work
	${}^{2}L^{\text{liq.}}_{\text{Co,Fe,Zr}} = -137419.3 + 83.1767T$	This work
fcc_A1	${}^{0}L^{\text{fcc\_A1}}_{\text{Co,Fe}} = -9112.0 + 3.3000T$	12
	${}^{2}L^{\text{fcc\_A1}}_{\text{Co,Fe}} = +1667.0$	12
	${}^{0}T^{\text{fcc\_A1}}_{c\text{Co,Fe}} = +283$	12
	${}^{2}T^{\text{fcc\_A1}}_{c\text{Co,Fe}} = +879$	12
	${}^{0}\beta^{\text{fcc\_A1}}_{\text{Co,Fe}} = +8.9$	12
	${}^{2}\beta^{\text{fcc\_A1}}_{\text{Co,Fe}} = -3.9$	12
	${}^{0}L^{\text{fcc\_A1}}_{\text{Fe,Zr}} = -16847.9 - 3.5600T$	14
bcc_A2 (disordered part of B2)	$G^{\text{bcc\_A2}}_{\text{Va}} = +30T$	12
	${}^{0}L^{\text{bcc\_A2}}_{\text{Co,Va}} = +126184.0$	12
	${}^{0}L^{\text{bcc\_A2}}_{\text{Fe,Va}} = +150000.0$	12
	${}^{0}L^{\text{bcc\_A2}}_{\text{Zr,Va}} = +150000.0$	This work
	${}^{0}L^{\text{bcc\_A2}}_{\text{Co,Fe}} = -20205.0 + 14.8000T + 0.9845T \times \ln T - 0.0076434T^{2}$	12
	${}^{2}L^{\text{bcc\_A2}}_{\text{Co,Fe}} = +1316.0$	12
	${}^{0}T^{\text{bcc\_A2}}_{c\text{Co,Fe}} = +590$	12
	${}^{0}\beta^{\text{bcc\_A2}}_{\text{Co,Fe}} = +1.5$	12
	${}^{2}\beta^{\text{bcc\_A2}}_{\text{Co,Fe}} = -0.6$	12
	${}^{0}L^{\text{bcc\_A2}}_{\text{Co,Zr}} = -79348.0 + 23.3360T$	13
	${}^{0}L^{\text{bcc\_A2}}_{\text{Fe,Zr}} = -33690.0 + 8.7700T$	14
	${}^{1}L^{\text{bcc\_A2}}_{\text{Fe,Zr}} = -11176.6 + 7.6300T$	14
bcc_B2	$G^{\text{bcc\_B2}}_{\text{Co:Fe}} = G^{\text{bcc\_B2}}_{\text{Fe:Co}} = -1245.0 - 1.8900T$	12
	${}^{0}L^{\text{bcc\_B2}}_{\text{Fe:Co,Fe}} = {}^{0}L^{\text{bcc\_B2}}_{\text{Co,Fe:Fe}} = -872.0$	12
	$T^{\text{bcc\_B2}}_{c\text{Co:Fe}} = T^{\text{bcc\_B2}}_{c\text{Fe:Co}} = +370$	12
	$\beta^{\text{bcc\_B2}}_{\text{Co:Fe}} = \beta^{\text{bcc\_B2}}_{\text{Fe:Co}} = +0.14$	12
	${}^{0}T^{\text{bcc\_B2}}_{c\text{Co:Co,Fe}} = {}^{0}T^{\text{bcc\_B2}}_{c\text{Co,Fe:Co}} = {}^{0}T^{\text{bcc\_B2}}_{c\text{Fe:Co,Fe}} = {}^{0}T^{\text{bcc\_B2}}_{c\text{Co,Fe:Fe}} = -370$	12
	$G^{\text{bcc\_B2}}_{\text{Co:Zr}} = G^{\text{bcc\_B2}}_{\text{Zr:Co}} = -34937.0 - 3.7845T$	This work
	${}^{0}L^{\text{bcc\_B2}}_{\text{Zr:Co,Zr}} = {}^{0}L^{\text{bcc\_B2}}_{\text{Co,Zr:Zr}} = +20000.0$	This work
	$G^{\text{bcc\_B2}}_{\text{Fe:Zr}} = G^{\text{bcc\_B2}}_{\text{Zr:Fe}} = -29679.4 + 5.6578T$	This work
	${}^{0}L^{\text{bcc\_B2}}_{\text{Zr:Co,Fe}} = {}^{0}L^{\text{bcc\_B2}}_{\text{Co,Fe:Zr}} = -2816.9 - 6.9789T$	This work
	${}^{1}L^{\text{bcc\_B2}}_{\text{Zr:Co,Fe}} = {}^{1}L^{\text{bcc\_B2}}_{\text{Co,Fe:Zr}} = +4346.2 - 8.1181T$	This work
	${}^{0}T^{\text{bcc\_B2}}_{c\text{Zr:Co,Fe}} = {}^{0}T^{\text{bcc\_B2}}_{c\text{Co,Fe:Zr}} = -370$	This work

Table 4 continued

Phase	Thermodynamic parameters	References
hcp_A3	${}^{0}L^{\mathrm{hcp\_A3}}_{\mathrm{Co,Fe}} = -8500.0 + 7.0000T$	12
	${}^{1}L^{\mathrm{hcp\_A3}}_{\mathrm{Co,Fe}} = -800.0$	12
	${}^{0}T^{\mathrm{hcp\_A3}}_{c\mathrm{Co,Fe}} = -253$	12
	${}^{2}T^{\mathrm{hcp\_A3}}_{c\mathrm{Co,Fe}} = +1494$	12
	${}^{0}\beta^{\mathrm{hcp\_A3}}_{\mathrm{Co,Fe}} = -0.78$	12
	${}^{2}\beta^{\mathrm{hcp\_A3}}_{\mathrm{Co,Fe}} = +1.54$	12
	${}^{0}L^{\mathrm{hcp\_A3}}_{\mathrm{Co,Zr}} = -43000.0$	This work
	${}^{0}L^{\mathrm{hcp\_A3}}_{\mathrm{Fe,Zr}} = +5769.6$	14
$Co_{11}Zr_2$	$G^{\mathrm{Co_{11}Zr_2}}_{\mathrm{Co:Zr}} = +11\mathrm{GHSER_{Co}} + 2\mathrm{GHSER_{Zr}} - 405002.0 + 89.7390T$	13
	$G^{\mathrm{Co_{11}Zr_2}}_{\mathrm{Fe:Zr}} = +11\mathrm{GHSER_{Fe}} + 2\mathrm{GHSER_{Zr}} - 240011.8 + 55.2912T$	This work
	${}^{0}L^{\mathrm{Co_{11}Zr_2}}_{\mathrm{Co,Fe:Zr}} = +526887.8 - 378.7426T$	This work
$(Co,Fe)_{23}Zr_6$	$G^{\mathrm{(Co,Fe)_{23}Zr_6}}_{\mathrm{Co:Zr}} = +23\mathrm{GHSER_{Co}} + 6\mathrm{GHSER_{Zr}} - 1026600 + 162.4000T$	13
	$G^{\mathrm{(Co,Fe)_{23}Zr_6}}_{\mathrm{Fe:Zr}} = +23\mathrm{GHSER_{Fe}} + 6\mathrm{GHSER_{Zr}} - 680411.0 + 123.3419T$	This work
	${}^{0}L^{\mathrm{(Co,Fe)_{23}Zr_6}}_{\mathrm{Co,Fe:Zr}} = -69757.7 - 92.4928T$	This work
	${}^{1}L^{\mathrm{(Co,Fe)_{23}Zr_6}}_{\mathrm{Co,Fe:Zr}} = +338832.1 - 167.8839T$	This work
	${}^{2}L^{\mathrm{(Co,Fe)_{23}Zr_6}}_{\mathrm{Co,Fe:Zr}} = -49983.2$	This work
λ_2	$G^{\lambda_2}_{\mathrm{Co:Co}} = +3\mathrm{GHSER_{Co}} + 15000.0$	13
	$G^{\lambda_2}_{\mathrm{Co:Zr}} = +2\mathrm{GHSER_{Co}} + \mathrm{GHSER_{Zr}} - 112008.0 + 2.9100T$	13
	$G^{\lambda_2}_{\mathrm{Zr:Co}} = +G^{\lambda_2}_{\mathrm{Co:Co}} + G^{\lambda_2}_{\mathrm{Zr:Zr}} - G^{\lambda_2}_{\mathrm{Co:Zr}}$	13
	$G^{\lambda_2}_{\mathrm{Zr:Zr}} = +3\mathrm{GHSER_{Zr}} + 15000.0$	13
	${}^{0}L^{\lambda_2}_{\mathrm{Co:Co,Zr}} = -111925.0 + 58.0000T$	This work
	${}^{1}L^{\lambda_2}_{\mathrm{Co:Co,Zr}} = +45000.0$	13
	$G^{\lambda_2}_{\mathrm{Fe:Fe}} = +3\mathrm{GHSER_{Fe}} + 15000.0$	14
	$G^{\lambda_2}_{\mathrm{Co:Fe}} = +2\mathrm{GHSER_{Co}} + \mathrm{GHSER_{Fe}} + 15000.0$	This work
	$G^{\lambda_2}_{\mathrm{Fe:Co}} = +G^{\lambda_2}_{\mathrm{Co:Co}} + G^{\lambda_2}_{\mathrm{Fe:Fe}} - G^{\lambda_2}_{\mathrm{Co:Fe}}$	This work
	$G^{\lambda_2}_{\mathrm{Fe:Zr}} = -112156.0 + 438.6000T - 79.1130T \times \ln T - 0.0068T^2 + 330106T^{-1}$	14
	$G^{\lambda_2}_{\mathrm{Zr:Fe}} = -G^{\lambda_2}_{\mathrm{Fe:Zr}} + 30000.0$	14
	${}^{0}L^{\lambda_2}_{\mathrm{Fe:Fe,Zr}} = -23000.0 + 22.5000T$	14
	${}^{0}L^{\lambda_2}_{\mathrm{Fe,Zr:Zr}} = +56000.0$	14
	$T^{\lambda_2}_{c\mathrm{Fe:Zr}} = +585$	14
	$\beta^{\lambda_2}_{\mathrm{Fe:Zr}} = +1.4$	14
	${}^{0}L^{\lambda_2}_{\mathrm{Co,Fe:Zr}} = -92413.7 + 33.3198T$	This work
	${}^{1}L^{\lambda_2}_{\mathrm{Co,Fe:Zr}} = -36207.3 + 16.6599T$	This work
$(Co,Fe)_1Zr_2$	$G^{\mathrm{(Co,Fe)_1Zr_2}}_{\mathrm{Co:Zr}} = +\mathrm{GHSER_{Co}} + 2\mathrm{GHSER_{Zr}} - 95360.2 + 10.4660T$	This work
	$G^{\mathrm{(Co,Fe)_1Zr_2}}_{\mathrm{Fe:Zr}} = +\mathrm{GHSER_{Fe}} + 2\mathrm{GHSER_{Zr}} - 44258.8 - 2.7322T$	14
	${}^{0}L^{\mathrm{(Co,Fe)_1Zr_2}}_{\mathrm{Co,Fe:Zr}} = +86785.1 - 73.2012T$	This work
	${}^{1}L^{\mathrm{(Co,Fe)_1Zr_2}}_{\mathrm{Co,Fe:Zr}} = +4496.8$	This work

Table 4 continued

Phase	Thermodynamic parameters	References
$(Co,Fe)_1Zr_3$	$G^{(Co,Fe)_1Zr_3}_{Co:Zr} = +GHSER_{Co} + 3GHSER_{Zr} - 100563.2 + 13.9980T$	This work
	$G^{(Co,Fe)_1Zr_3}_{Fe:Zr} = -80910.0 + 519.9000T - 97.8640T \times \ln T - 0.0141T^2 + 144141T^{-1}$	14
λ_3	$G^{\lambda_3}_{Fe:Fe} = +3GHSER_{Fe} + 15000.0$	14
	$G^{\lambda_3}_{Fe:Zr} = -113009.0 + 440.2000T - 79.1130T \times \ln T - 0.0068T^2 + 330106T^{-1}$	14
	$G^{\lambda_3}_{Zr:Fe} = -G^{\lambda_3}_{Fe:Zr} + 30000.0$	14
	$G^{\lambda_3}_{Zr:Zr} = +3GHSER_{Zr} + 15000.0$	14
	${}^0L^{\lambda_3}_{Fe:Fe,Zr} = -1533.1 + 3.0950T$	14
	${}^0L^{\lambda_3}_{Fe,Zr:Zr} = +56000.0$	14
	$G^{\lambda_3}_{Co:Co} = +3GHSER_{Co} + 15000.0$	This work
	$G^{\lambda_3}_{Co:Fe} = +2GHSER_{Co} + GHSER_{Fe} + 15000.0$	This work
	$G^{\lambda_3}_{Fe:Co} = +G^{\lambda_3}_{Co:Co} + G^{\lambda_3}_{Fe:Fe} - G^{\lambda_3}_{Co:Fe}$	This work
	$G^{\lambda_3}_{Co:Zr} = +2GHSER_{Co} + GHSER_{Zr} - 97008.0 + 2.9100T$	This work
	$G^{\lambda_3}_{Zr:Co} = +G^{\lambda_3}_{Co:Co} + G^{\lambda_3}_{Zr:Zr} - G^{\lambda_3}_{Co:Zr}$	This work

homogeneity ranges.[11] Taking the Laves phase λ_2 as an example, its Gibbs energy is given as follows:

$$G_m^{\lambda_2} = \sum_r y_r' \sum_s y_s'' G_{r:s}^{\lambda_2} + RT(2\sum_r y_r' \ln y_r' + \sum_s y_s'' \ln y_s'') + {}^E G_m^{\lambda_2} \quad \text{(Eq 3)}$$

$${}^E G_m^{\lambda_2} = \sum_u \sum_v y_u' y_v' \sum_w \sum_j y_w''^{\,j} L_{u,v:w}^{\lambda_2} (y_u' - y_v')^j + \sum_u \sum_v y_u'' y_v'' \sum_w \sum_j y_w'^{\,j} L_{w:u,v}^{\lambda_2} (y_u'' - y_v'')^j \quad \text{(Eq 4)}$$

where y_*' and y_*'' are the site fractions of * (* = Co, Fe and Zr); $G_{r:s}^{\lambda_2}$ represent the Gibbs energy in its SER state, hcp_A3 for Co, bcc_A2 for Fe or hcp_A3 for Zr; ${}^jL_{u,v:w}^{\lambda_2}$ and ${}^jL_{w:u,v}^{\lambda_2}$ are the assessed jth interaction parameters in this work.

The triple-defect mechanism is important for bcc_B2 when considering its site ordering.[52] In order to combine with bcc_B2, the vacancies should occupy sites on each sublattice in bcc_A2. Two intermetallic phases CoFe and CoZr had the ordered bcc_B2 crystal structure and a single Gibbs energy function derived by Ansara et al.[53] was proposed to describe the disordered bcc_A2 and ordered bcc_B2 simultaneously:

$$\begin{aligned} G_m^{bcc} &= G_m^{bcc\_A2}(x_i) + \Delta G_m^{bcc\_B2}(y_i', y_i) \\ &= G_m^{bcc\_A2}(x_i) + G_m^{bcc\_B2}(y_i', y_i) - G_m^{bcc\_B2}(x_i) \end{aligned} \quad \text{(Eq 5)}$$

where $G_m^{\text{bcc\_A2}}(x_i)$ means the Gibbs energy of bcc_A2; $G_m^{bcc\_B2}(y_i', y_i)$ and $G_m^{\text{bcc\_B2}}(x_i)$ are the contribution of bcc_B2 and the one from bcc_A2 to bcc_B2, respectively. When $x_i = y_i' = y_i$ (i = Co, Fe, Va and Zr), the phase is bcc_A2, otherwise it would be bcc_B2.

4 Result and Discussion

In the present work, the Thermo-Calc software package[54] is used for optimizing the Co–Zr and Co–Fe–Zr systems. The crystal structures and thermodynamic models of each phase are presented in Table 1.

In the optimization process, $Fe_{23}Zr_6$ is treated as a metastable phase in the Fe–Zr system according to the detailed experimental results[40]. And the value a of $G^{(Co,Fe)_{23}Zr_6}_{Fe:Zr}$(=$a + bT$) is set to − 680411.0 based on the reported enthalpy of formation from the ab-initio calculations[43], and the value b is set to a suitable one to satisfy the metastable state in the Fe–Zr system.

Figure 3 and Table 2 present the calculated phase diagram and invariant reactions of the Co–Zr system superimposed with the previous work[13] and experimental

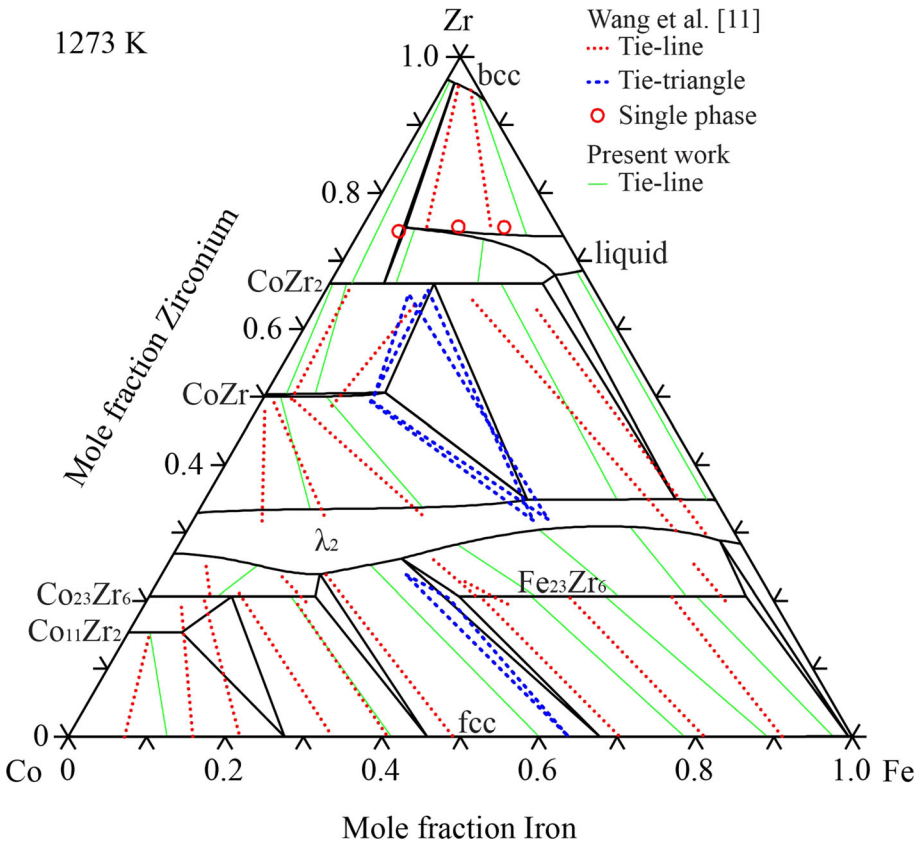

Fig. 4 Calculated isothermal section at 1273 K of the Co–Fe–Zr system compared with the experimental data[11].

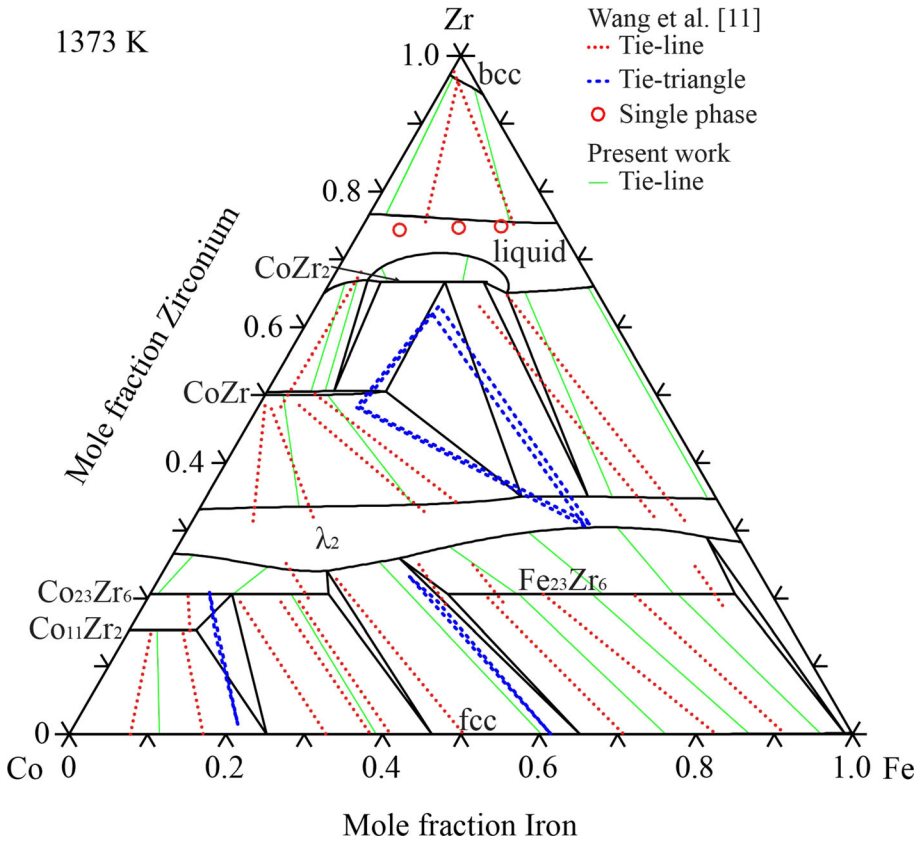

Fig. 5 Calculated isothermal section at 1373 K of the Co–Fe–Zr system compared with the experimental data[11].

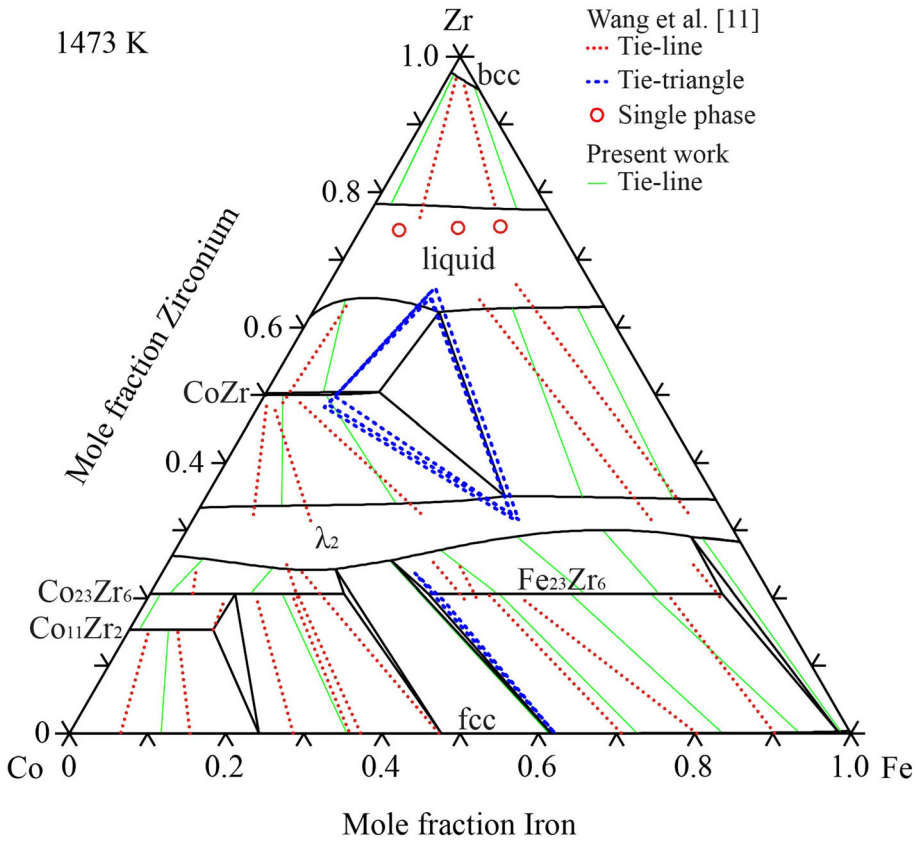

Fig. 6 Calculated isothermal section at 1473 K of the Co–Fe–Zr system compared with the experimental data[11].

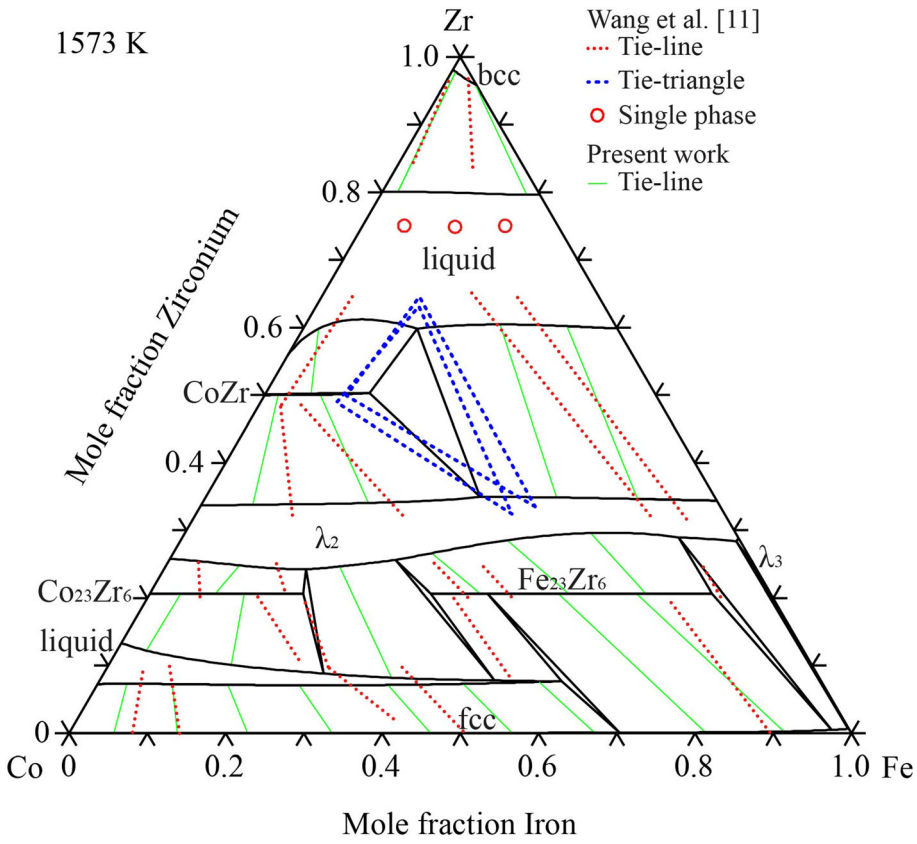

Fig. 7 Calculated isothermal section at 1573 K of the Co–Fe–Zr system compared with the experimental data[11].

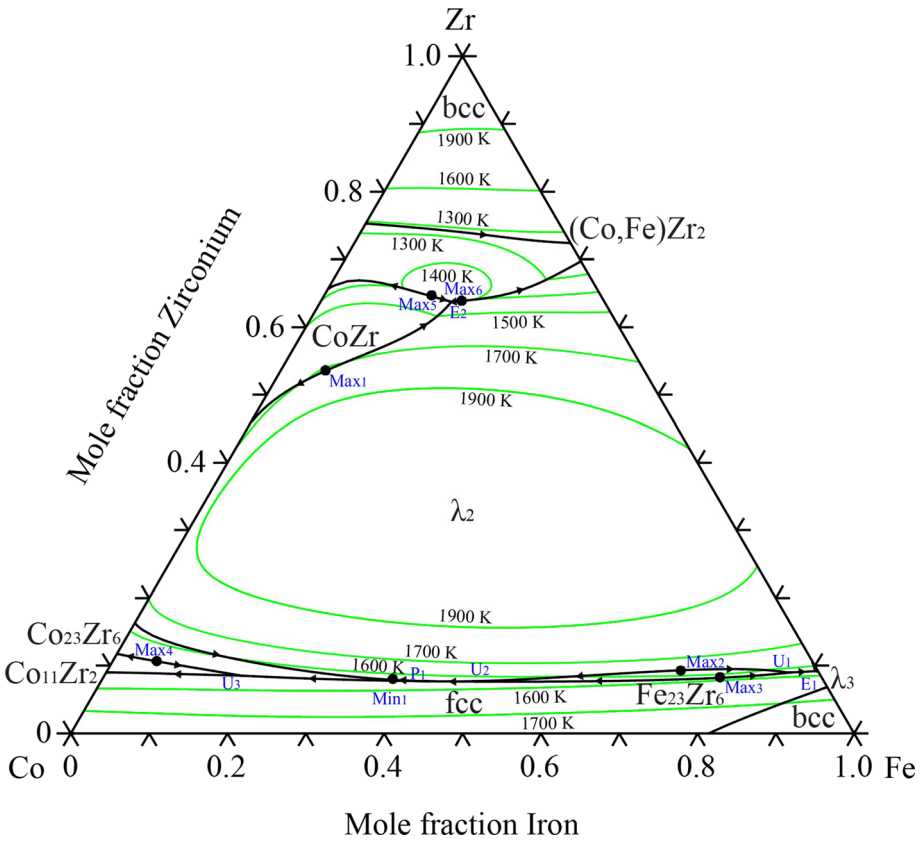

Fig. 8 Calculated liquidus surface projection of the Co–Fe–Zr system.

Table 5 Predicted invariant reactions involving liquid phase in the Co–Fe–Zr system

Reaction	Type	*T*,K	Liquid compositions at.%		
			Co	Fe	Zr
liq. + $\lambda_2 \leftrightarrow$ CoZr	p_1, Max_1	1705	0.407	0.057	0.536
liq. + $\lambda_2 \leftrightarrow Fe_{23}Zr_6$	p_2, Max_2	1627	0.175	0.732	0.093
liq. $\leftrightarrow Fe_{23}Zr_6$ + fcc(Co,Fe)	e_1, Max_3	1587	0.130	0.787	0.083
liq. $\leftrightarrow \lambda_2 + Co_{23}Zr_6$	e_2, Min_1	1556	0.522	0.400	0.078
liq. $\leftrightarrow Co_{23}Zr_6 + Co_{11}Zr_2$	e_3, Max_4	1543	0.837	0.056	0.107
liq. + CoZr $\leftrightarrow$ (Co,Fe)Zr_2	p_3, Max_5	1408	0.217	0.137	0.646
liq. + $\lambda_2 \leftrightarrow$ (Co,Fe)Zr_2	p_4, Max_6	1402	0.184	0.177	0.639
liq. + $Fe_{23}Zr_6 \leftrightarrow \lambda_2$ + fcc(Co,Fe)	U_1	1579	0.038	0.872	0.090
liq. $\leftrightarrow \lambda_2 + \lambda_3$ + fcc(Co,Fe)	E_1	1577	0.003	0.905	0.092
liq. + $Fe_{23}Zr_6 \leftrightarrow \lambda_2$ + fcc(Co,Fe)	U_2	1559	0.479	0.444	0.077
liq. + λ_2 + fcc(Co,Fe) $\leftrightarrow Co_{23}Zr_6$	P_1	1557	0.506	0.417	0.077
liq. + $Co_{23}Zr_6 \leftrightarrow Co_{11}Zr_2$+ fcc(Co,Fe)	U_3	1525	0.740	0.174	0.086
liq. $\leftrightarrow$ (Co,Fe)Zr_2 + CoZr + λ_2	E_2	1401	0.195	0.166	0.639

data.[24, 29–32] In comparison with the former work,[13] the low-temperature decomposition of $CoZr_3$ has been solved. The calculated enthalpies of formation of the Co–Zr compounds at 298 K in comparison with the previous work[13] and experimental data[33–37] are presented in Table 3. Nearly all the reported enthalpies of formation are well reproduced. The calculated enthalpy of formation of $CoZr_2$ is more positive than the reported one[13] to avoid the low-temperature decomposition of $CoZr_3$.

The Co–Fe–Zr thermodynamic parameters are summarized in Table 4. Figure. 4, 5, 6, 7 show the four calculated Co–Fe–Zr isothermal sections at 1273, 1373, 1473, and 1573 K together with the experimental data.[11] Most of the experimental information is well reproducible, but there

still exist a few acceptable discrepancies. The calculated phase boundaries of the liquid phase at 1573 K show large inconsistency with the experimental data[11] probably because of the experimental uncertainty at a very high temperature. With the stability limit of $CoZr_2$ at 1473 K, the two-phase region $CoZr_2 + \lambda_2$ at 1373 K is impossible to fully meet the experimental data.[11] The three-phase regions $Co_{23}Zr_6 + Co_{11}Zr_2 +$ fcc(Co,Fe) at 1273 and 1373 K disagree with the experimental information.[11] Although great efforts were made, the value b of ${}^0L^{Co_{11}Zr_2}_{Co,Fe:Zr}$ ($=a + bT$) would need to be -60 J/(mol K) to fit this three-phase region. This value leads to the occurrence of $Co_{11}Zr_2$ at 1573 K and cannot be accepted in this work. Therefore, further studies are recommended to determine the phase relations about $Co_{11}Zr_2$ below 1373 K. Additionally, the tie-lines $\lambda_2 + Co_{23}Zr_6$ at 1273, 1373, 1473, and 1573 K have some differences from the experimental data,[11] which is due to the experimental homogeneity range and corresponding Gibbs energy of λ_2.

The calculated liquidus surface projection and corresponding invariant reactions of the Co–Fe–Zr system are also shown in Fig. 8 and Table 5.

5 Conclusion

In the current study, the thermodynamic descriptions of the Co–Zr and Co–Fe–Zr systems have been carried out using the CALPHAD approach in accordance with the experimental phase equilibria and thermochemical information. There is a satisfactory agreement between the experimental and calculated results. The reliable Co–Fe–Zr thermodynamic parameters are first acquired, which can be used as a cost-effective tool for materials design and processing.

Acknowledgment This work was supported by Scientific Research Starting Foundation for Advanced Talents of Jiangxi University of Science and Technology (Grant No. 205200100063).

References

1. F. Wang, R. Li, C. Ding, W. Tang, Y. Wang, S. Xu, R. Yu, and Y. Wu, F. Wang, R. Li, C. Ding, W. Tang, Y. Wang, S. Xu, R. Yu, and Y. Wu, Recent Progress On The Hydrogen Storage Properties of ZrCo-Based Alloys Applied in International Thermonuclear Experimental Reactor (ITER), *Prog. Nat. Sci. Mater.*, 2017, **27**(1), p 58–65
2. R.A. Jat, R. Singh, S.C. Parida, A. Das, R. Agarwal, S.K. Mukerjee, and K.L. Ramakumar, R.A. Jat, R. Singh, S.C. Parida, A. Das, R. Agarwal, S.K. Mukerjee, and K.L. Ramakumar, Structural and Hydrogen Isotope Storage Properties of Zr–Co–Fe Alloy, *Int. J. Hydrogen Energy*, 2015, **40**(15), p 5135–5143
3. C. Xie, W. Li, J. Luo, Y. Yang, and S. Li, C. Xie, W. Li, J. Luo, Y. Yang, and S. Li, Development of MAgnetic and Ductile Fe-Co-Zr-Mo-Cr Glassy Alloy Without Metalloid Elements, *J. Non-Cryst. Solids*, 2018, **482**, p 213–216
4. P. Yu, J.Z. Zhang, and L. Xia, P. Yu, J.Z. Zhang, and L. Xia, $Fe_{87}Zr_7B_4Co_2$ Amorphous Alloy with Excellent Magneto-caloric Effect Near Room Temperature, *Intermetallics*, 2018, **95**, p 85–88
5. A.P. Srivastava, D.A. Babu, A. Verma, A.A. Deshmukh, A. Kaushal, and U.A. Palikundwar, Understanding the Effect of Hf on Thermal Stability and Glass Forming Ability of $Fe_{572}Co_{308}Zr_{7-x}Hf_xB_4Cu1$ (x = 3, 5, and 7) Metallic Glasses, *J. Non-Cryst. Solids*, 2019. https://doi.org/10.1016/j.jnoncrysol.2018.09.016
6. K. Kotynia, P. Pawlik, K. Filipecka, and J. Filipecki, K. Kotynia, P. Pawlik, K. Filipecka, and J. Filipecki, Calorimetric and Structural Analysis of the Zr–Fe–Co–B–Mo–W Amorphous Alloys Doped With Gadolinium, *J. Alloy. Compd.*, 2020, **842**, p 155940
7. P. Gong, S. Wang, F. Li, and X. Wang, P. Gong, S. Wang, F. Li, and X. Wang, Kinetics of Glass Transition and Crystallization of a $Zr_{40}Hf_{10}Ti_4Y_1Al_{10}Cu_{25}Ni_7Co_2Fe_1$ Bulk Metallic Glass with High Mixing Entropy, *Metall. Mater. Trans. A*, 2018, **49**, p 2918–2928
8. J. Liu, Z. Xing, H. Wang, X. Cui, G. Jin, and B. Xu, J. Liu, Z. Xing, H. Wang, X. Cui, G. Jin, and B. Xu, Microstructure and Fatigue Damage Mechanism of Fe–Co–Ni–Al–Ti–Zr High-entropy Alloy Film by Nanoscale Dynamic Mechanical Analysis, *Vacuum*, 2019, **159**, p 516–523
9. C. Chen, H. Zhang, Y. Fan, W. Zhang, R. Wei, S. Guan, T. Wang, B. Kong, T. Zhang, and F. Li, C. Chen, H. Zhang, Y. Fan, W. Zhang, R. Wei, S. Guan, T. Wang, B. Kong, T. Zhang, and F. Li, Crystallization and Corrosion Resistance of Zr–Ti–Y–Al–Cu–Ni–Co–Fe Complex Multi-component Bulk Metallic Glasses, *Intermetallics*, 2020, **118**, p 106688
10. S.M. Hoque, S.K. Makineni, A. Pal, S.A. Rahman, S. Hossain, R. Islam, P. Ayyub, and K. Chattopadhyay, S.M. Hoque, S.K. Makineni, A. Pal, S.A. Rahman, S. Hossain, R. Islam, P. Ayyub, and K. Chattopadhyay, Two Phase Ferromagnetic Composites in Co-Zr and Co-Zr-Fe Systems Containing Anti-Phase Domain Imparting Very High Strength, *Mater. Res. Bull.*, 2018, **97**, p 61–70
11. C.P. Wang, Y. Yu, H.H. Zhang, H.F. Hu, and X.J. Liu, C.P. Wang, Y. Yu, H.H. Zhang, H.F. Hu, and X.J. Liu, Experimental Determination of the Phase Equilibria in the Co–Fe–Zr Ternary System, *J. Alloy. Compd.*, 2011, **509**(13), p 4470–4477
12. J. Wang, X. Lu, N. Zhu, and W. Zheng, J. Wang, X. Lu, N. Zhu, and W. Zheng, Thermodynamic and Diffusion kinetic Studies of the Fe-Co System, *Calphad*, 2017, **58**, p 82–100
13. P. Agraval, L. Dreval, M. Turchanin, and T. Velikanova, P. Agraval, L. Dreval, M. Turchanin, and T. Velikanova, Thermodynamic Assessment of the Co-Zr System, *J. Phase Equilib. Diffus.*, 2020, **41**, p 491–499
14. I. Saenko, A. Kupravaa, A. Udovsky, and O. Fabrichnaya, I. Saenko, A. Kupravaa, A. Udovsky, and O. Fabrichnaya, Heat Capacity Measurement of Zr_2Fe and Thermodynamic Re-assessment of the Fe–Zr System, *Calphad*, 2019, **66**, p 101625
15. A.F. Guillermet, A.F. Guillermet, Critical Evaluation of the Thermodynamic Properties of the Iron-Cobalt System, *High Temp. High Press.*, 1987, **19**(5), p 477–499
16. I. Ohnuma, H. Enoki, O. Ikeda, R. Kainuma, H. Ohtani, B. Sundman, and K. Ishida, I. Ohnuma, H. Enoki, O. Ikeda, R. Kainuma, H. Ohtani, B. Sundman, and K. Ishida, Phase Equilibria in the Fe–Co Binary System, *Acta Mater.*, 2002, **50**(2), p 379–393
17. M.A. Turchanin, L.A. Dreval, A.R. Abdulov, and P.G. Agraval, M.A. Turchanin, L.A. Dreval, A.R. Abdulov, and P.G. Agraval, Mixing Enthalpies of Liquid Alloys and Thermodynamic

Assessment of the Cu–Fe–Co System, *Powd. Metall. Met. Ceram.*, 2011, **50**(1–2), p 98–116
18. M.F. Collins, and J.B. Forsyth, M.F. Collins, and J.B. Forsyth, The Magnetic Moment Distribution in Some Transition Metal Alloys, *Philos. Mag.*, 1963, **8**(87), p 401–410
19. D.I. Bardos, D.I. Bardos, Mean Magnetic Moments in bcc Fe-Co Alloys, *J. Appl. Phys.*, 1969, **40**(3), p 1371–1372
20. M. Kogachi, N. Tadachi, H. Kohata, and H. Ishibashi, M. Kogachi, N. Tadachi, H. Kohata, and H. Ishibashi, Magnetism and Point Defect in B2-type CoFe Alloys, *Intermetallics*, 2005, **13**(5), p 535–542
21. T. Chart, and F. Putland, T. Chart, and F. Putland, A Thermodynamically Calculated Phase Diagram for the Co–Cr–Zr System, *Calphad*, 1979, **3**(1), p 9–18
22. N. Saunders, and A.P. Miodownik, N. Saunders, and A.P. Miodownik, Thermodynamic Aspects of Amorphous Phase Formation, *J. Mater. Res.*, 1986, **1**(1), p 38–46
23. J. Bratberg, and B. Jansson, J. Bratberg, and B. Jansson, Thermodynamic Evaluation of the c-co-w-hf-zr System for Cemented Carbides Applications, *J. Phase Equilib. Diffus.*, 2006, **27**(3), p 213–219
24. X.J. Liu, H.H. Zhang, C.P. Wang, and K. Ishida, X.J. Liu, H.H. Zhang, C.P. Wang, and K. Ishida, Experimental Determination and Thermodynamic Assessment of the Phase Diagram in the Co–Zr System, *J. Alloy. Compd.*, 2009, **482**(1–2), p 99–105
25. Yu.O. Esin, OYu. Sidorov, M.G. Valishev, and P.V. Geld, Yu.O. Esin, OYu. Sidorov, M.G. Valishev, and P.V. Geld, The Enthalpies of Formation of Molten Zirconium Alloys with Cobalt, *TVT*, 1989, **27**(2), p 394–396
26. R. Lück, H. Wang, and B. Predel, R. Lück, H. Wang, and B. Predel, Calorimetric Determination of the Mixing Enthalpy of Liquid Cobal-Zirconium Alloys, *Z. Anorg. Allg. Chem.*, 1993, **619**(3), p 447–452
27. M.A. Turchanin, and P.G. Agraval, M.A. Turchanin, and P.G. Agraval, Enthalpies of Mixing of Titanium, Zirconium and Hafnium Liquid Alloys with Cobalt, *Rasplavy*, 2002, **2**, p 8–16
28. A. Durga, and K.C. Hari Kumar, A. Durga, and K.C. Hari Kumar, Thermodynamic Optimization of the Co–Zr System, *Calphad*, 2010, **34**(2), p 200–205
29. Kosorukova, T., Agraval, P., Ivanchenko, V., Turchanin, M, (2010) Experimental reinvestigations and thermodynamic assessment of the Co–Zr system, XI International Conference on Crystal Chemistry of Intermetallic Compounds, May 30–June 2, National University of Lviv, p 52
30. O.L. Semenova, V.M. Petyukh, and O.S. Fomichev, O.L. Semenova, V.M. Petyukh, and O.S. Fomichev, The Constitution of Co–Zr Phase Diagram, *Powder Metall. Met. Ceram.*, 2016, **54**(9–10), p 583–589
31. W.H. Pechin, D.E. Williams, and W.L. Larsen, W.H. Pechin, D.E. Williams, and W.L. Larsen, The Zirconium-Cobalt Alloy System, *Trans. ASM*, 1964, **57**, p 464–473
32. S.K. Bataleva, V.V. Kuprina, V.V. Burnasheva, V.Y. Markiv, G.N. Ronami, and S.M. Kurnetsova, S.K. Bataleva, V.V. Kuprina, V.V. Burnasheva, V.Y. Markiv, G.N. Ronami, and S.M. Kurnetsova, Phase Diagram of Cobalt– Zirconium System, *Moscow Univ. Chem. Bull.*, 1970, **25**(5), p 33–36
33. J.C. Gachon, and J. Hertz, J.C. Gachon, and J. Hertz, Enthalpies of Formation of Binary Phases in the Systems FeTi, FeZr, CoTi, CoZr, NiTi, and NiZr, by Direct Reaction Calorimetry, *Calphad*, 1983, **7**(1), p 1–12
34. Q. Guo, and O.J. Kleppa, Q. Guo, and O.J. Kleppa, Standard Enthalpies Of Formation Of Some Alloys Formed Between Group IV Elements and Group VIII Elements, Determined by High-Temperature Direct Synthesis Calorimetry II Alloys of (Ti, Zr, Hf) with (Co, Ni), *J Alloy Compd*, 1998, **269**(1–2), p 181–186
35. P.A. Gomozov, Y.V. Zasypalov, and B.M. Mogutnov, P.A. Gomozov, Y.V. Zasypalov, and B.M. Mogutnov, Enthalpies of Formation Of Intermetallic Compounds with CsCl Structure (CoTi, CoZr, CoAl, NiTi), *Russ. J. Phys. Chem.*, 1986, **60**(8), p 1122–1124
36. R. Klein, P.A.G. O'Hare, and I. Jacob, R. Klein, P.A.G. O'Hare, and I. Jacob, Standard Molar Enthalpies of Formation of Alloys in the Pseudobinary System $Zr(Al_xCo_{1-x})_2$ at the Temperature 298.15 K, *J Alloy Compd*, 1997. https://doi.org/10.1016/S0925-8388(97)00226-0
37. P.R. Ohodnicki Jr., N.C. Cates, D.E. Laughlin, M.E. McHenry, and M. Widom, P.R. Ohodnicki Jr., N.C. Cates, D.E. Laughlin, M.E. McHenry, and M. Widom, Ab Initio Theoretical Study Of Magnetization And Phase Stability of the (Fe Co, Ni)23B6 and (Fe Co, Ni)23Zr6 Structures of Cr23C6 and Mn23Th6 Prototypes, *Phys. Rev. B*, 2008, **78**(14), p 144414
38. C. Servant, C. Gueneau, and I. Ansara, C. Servant, C. Gueneau, and I. Ansara, Experimental and Thermodynamic Assessment of the Fe–Zr System, *J. Alloy. Compd.*, 1995, **220**(1–2), p 19–26
39. M. Jiang, K. Oikawa, T. Ikeshoji, L. Wulff, and K. Ishida, M. Jiang, K. Oikawa, T. Ikeshoji, L. Wulff, and K. Ishida, Thermodynamic Calculations of Fe-Zr and Fe-Zr-C Systems, *J. Phase Equilib.*, 2001, **22**(4), p 406–417
40. F. Stein, G. Sauthoff, and M. Palm, F. Stein, G. Sauthoff, and M. Palm, Experimental Determination Of Intermetallic Phases, Phase Equilibria, And Invariant Reaction Temperatures in the Fe-Zr System, *J. Phase Equilib.*, 2002, **23**(6), p 480–494
41. C. Guo, Z. Du, C. Li, B. Zhang, and M. Tao, C. Guo, Z. Du, C. Li, B. Zhang, and M. Tao, Thermodynamic Description of the Al–Fe–Zr System, *Calphad*, 2008, **32**(4), p 637–649
42. Y. Yang, L. Tan, H. Bei, and J.T. Busby, Y. Yang, L. Tan, H. Bei, and J.T. Busby, Thermodynamic Modeling And Experimental Study of the Fe–Cr–Zr System, *J. Nucl. Mater.*, 2013, **441**(1–3), p 190–202
43. H. Lu, N. Zou, X. Zhao, J. Shen, X. Lu, and Y. He, H. Lu, N. Zou, X. Zhao, J. Shen, X. Lu, and Y. He, Thermodynamic Investigation of the Zr-Fe-Nb System and its Applications, *Intermetallics*, 2017, **88**, p 91–100
44. K. Ali, A. Arya, P.S. Ghosh, and G.K. Dey, K. Ali, A. Arya, P.S. Ghosh, and G.K. Dey, A First Principles Study of Cohesive, Elastic and Electronic Properties Of Binary Fe–Zr Intermetallics, *Comp. Mater. Sci.*, 2016, **112**, p 52–66
45. K. Ali, P.S. Ghosh, and A. Arya, K. Ali, P.S. Ghosh, and A. Arya, A DFT Study of Structural, Elastic and Lattice Dynamical Properties of Fe_2Zr and $FeZr_2$ Intermetallics, *J. Alloy. Compd.*, 2017, **723**(5), p 611–619
46. B.O. Mukhamedov, I. Saenko, A.V. Ponomareva, M.J. Kriegel, A. Chugreev, A. Udovsky, O. Fabrichnaya, and I.A. Abrikosov, B.O. Mukhamedov, I. Saenko, A.V. Ponomareva, M.J. Kriegel, A. Chugreev, A. Udovsky, O. Fabrichnaya, and I.A. Abrikosov, Thermodynamic and Physical Properties Of Zr_3fe And $Zrfe_2$ Intermetallic Compounds, *Intermetallics*, 2019, **109**, p 189–196
47. L.A. Panteleimonov, O.G. Burtseva, and V.V. Zubenko, L.A. Panteleimonov, O.G. Burtseva, and V.V. Zubenko, The Iron-Cobalt-Zirconium System, *Moscow Univ. Chem. Bull.*, 1981, **36**(6), p 89–90
48. I.V. Mishenina, E.F. Kazakova, E.M. Sokolovskaya, and N.Y. Tolmachiova, I.V. Mishenina, E.F. Kazakova, E.M. Sokolovskaya, and N.Y. Tolmachiova, Isothermal Cross-Section Of Phase Diagram of the Fe-Co-Zr System at 770 K, *Moscow Univ. Chem. Bull.*, 1996, **51**(1), p 52–54
49. SGTE Pure Elements (Unary) Database, Version 5.1, ⟨https://www.thermocalc.com/academia/researchers/assessment-of-thermodynamic-data/⟩, visited July 2 2020.
50. O. Redlich, and A.T. Kister, O. Redlich, and A.T. Kister, Algebraic Representation Of Thermodynamic Properties and The Classification of Solutions, *Ind. Eng. Chem.*, 1948, **40**(2), p 345–348

51. M. Hillert, and M. Jarl, M. Hillert, and M. Jarl, A Model For Alloying Effects In Ferromagnetic Metals, *Calphad*, 1978, **2**(3), p 227–238
52. N. Dupin, and I. Ansara, N. Dupin, and I. Ansara, On The Sublattice Formalism Applied to the B2 Phase, *Z. Metallkd.*, 1999, **90**(1), p 76–85
53. I. Ansara, N. Dupin, H.L. Lukas, and B. Sundman, I. Ansara, N. Dupin, H.L. Lukas, and B. Sundman, Thermodynamic Assessment Of The Al–Ni System, *J. Alloy. Compd.*, 1997, **247**(1), p 20–30
54. B. Sundman, B. Jansson, and J.O. Andersson, B. Sundman, B. Jansson, and J.O. Andersson, The Thermo-Calc Databank System, *Calphad*, 1985, **9**(2), p 153–190